

Correlated positron–electron emission from surfaces

This article has been downloaded from IOPscience. Please scroll down to see the full text article.

2008 J. Phys.: Condens. Matter 20 442001

(<http://iopscience.iop.org/0953-8984/20/44/442001>)

View [the table of contents for this issue](#), or go to the [journal homepage](#) for more

Download details:

IP Address: 129.252.86.83

The article was downloaded on 29/05/2010 at 16:06

Please note that [terms and conditions apply](#).

FAST TRACK COMMUNICATION

Correlated positron–electron emission from surfaces

G A van Riessen, F O Schumann, M Birke, C Winkler and J Kirschner

Max Planck Institute of Microstructure Physics, Weinberg 2, 06120 Halle, Germany

E-mail: riessen@mpi-halle.mpg.de and schumann@mpi-halle.mpg.de

Received 27 August 2008, in final form 1 September 2008

Published 12 September 2008

Online at stacks.iop.org/JPhysCM/20/442001

Abstract

We studied positron–electron pair emission from a LiF(100) surface following excitation by a positron beam with a kinetic energy of 85 eV. We show for the first time that emission of time-correlated positron–electron pairs occurs.

1. Introduction

Intense experimental and theoretical effort has been invested over recent decades to understand the mutual interaction of electrons in a solid that underlie phenomena such as magnetism and superconductivity. In recent years it has been demonstrated that information about the correlation between a pair of electrons in the solid can be recovered from the observed momenta of the pair of electrons emitted from the surface upon photon or electron impact [1–10]. Experimental advances have only recently overcome the inherent challenge in such correlation spectroscopy that lies in the small probability of detecting two particles produced by a single event.

Interactions between electrons in a solid are due to Coulomb and exchange interactions, the role of which was discussed in seminal papers by Wigner and Seitz [11] and Slater [12]. Notably, we have been able to directly observe the so-called exchange–correlation hole [8–10], a direct manifestation of Coulomb and exchange interactions that leads to a region of reduced electron density surrounding each electron. As Slater pointed out, the two contributions to the exchange–correlation hole may be different. Disentangling their effects is possible when one of the interacting electrons is replaced with its antiparticle, the positron. As positrons and electrons are distinguishable particles the Pauli principle does not apply and their interaction is solely Coulombic. This can be realized experimentally by measuring the momenta of an electron and positron emitted from a surface upon positron impact.

The differences and common features of electron emission from metallic surfaces upon the impact of low energy

positrons or electrons has been discussed by Berakdar [13]. Berakdar also first considered theoretically positron–electron pair emission upon the impact of low energy positrons and diffraction of the positron–electron pair, illustrating how distinguishability of the electron and positron leads to differences between the angular distribution of electron–positron pair emission upon positron impact and electron–electron pair emission upon electron impact.

In order to establish the feasibility of studying angular distributions one has to establish that correlated positron–electron pair emission from a surface does occur. Further, it must be determined whether the pair emission occurs with significant probability. In this brief report we will demonstrate that this is indeed the case.

2. Experiment

The experiment was performed at the positron beamline NEPOMUC (NEutron induced POSitron source MUniCh) located at the research reactor FRM-II in Garching [14, 20]. A beam of moderated positrons with kinetic energy of 85 eV (with respect to the vacuum level) was magnetically guided to the end of the beamline. There the beam was extracted from the magnetic field through an aperture in a magnetic shield and focused by electrostatic optics onto a LiF(100) crystal. The crystal and optics were mounted in an UHV chamber. The positron beam at the sample was aligned and characterized using a multichannel plate detector with a phosphor screen that was positioned in the plane imaged by the transfer lenses of two hemispherical analyzers (Scienta R4000). The FWHM of the beam at the sample position was approximately 1 mm. The

primary positron flux was estimated to be $5 \times 10^4 \text{ s}^{-1}$ from the rate of positron annihilation at the sample measured using a pair of gamma detectors to detect in coincidence collinear gamma rays. This was the highest positron intensity achievable at the time. The energy width (FWHM) of the positron beam was estimated from the width of the elastic peak to be approximately 4 eV.

LiF(100) was chosen as a target for this experiment because, in contrast to metals, its wide band gap prohibits an electron emitted from the valence band from losing a continuous range of energy below the band gap energy by electronic excitations. Experience with electron pair emission upon electron impact has shown that this leads to a region of low inelastic contributions in the spectrum that improves the ability to distinguish pair emission from the valence band [8, 9, 15]. The interaction of positrons with LiF has also been studied [16, 17]. Furthermore, previous experience has shown that a clean LiF(100) is easily prepared and when held at 150 °C contamination accumulating on the surface in vacuum is minimal and electrostatic charging of the surface is effectively mitigated.

As illustrated in figure 1, the primary positron beam was directed along the LiF(100) surface normal. The electron–optical axes of the analyzer input lenses were symmetrically arranged in the scattering plane with a separation of 90° such that the angle with respect to the surface normal was 45° for each one. One analyzer was configured to detect electrons while the other was configured to detect positrons by reversing the polarity of the voltages applied to the lens elements and analyzer components. We optimized the voltages applied to the analyzer transfer lens elements to provide high transmission of low kinetic energy electrons or positrons with large pass energies. Although it is possible, for the present first experiment the lenses were operated in a mode that does not preserve the angular information of the detected particles. An energy range of approximately $\pm 5\%$ of the pass energy is measured simultaneously by using a spatially resolving detection scheme. With the analyzers set to a mean energy of 30 eV and a pass energy of 300 eV it was possible to detect electron–positron pairs for which the kinetic energy of the positron E_{e^+} and of the electron E_{e^-} were in the range 15–45 eV and the sum energy of the pair $E_{\text{sum}} = E_{e^+} + E_{e^-}$ was in the range 30–90 eV.

The detectors consisted of a pair of multichannel plates (MCP) in a chevron configuration together with a resistive anode. The same detection scheme was employed for electrons and positrons, except that for the detection of positrons the front MCP was negatively biased with respect to a mesh placed in front of it. There is little information available regarding the efficiency of positron detection by MCP, although there are various reports of using channeltron detectors for positrons (e.g. Goodyear and Coleman [18]). It is reasonable to assume that it is comparable to the electron detection efficiency because the detected signal in both cases results from an electron avalanche initiated with significant probability by secondary electrons when the electron or positron impacts the MCP surface.

A conventional coincidence circuit was used to ensure that only positron–electron pairs were detected and to distinguish

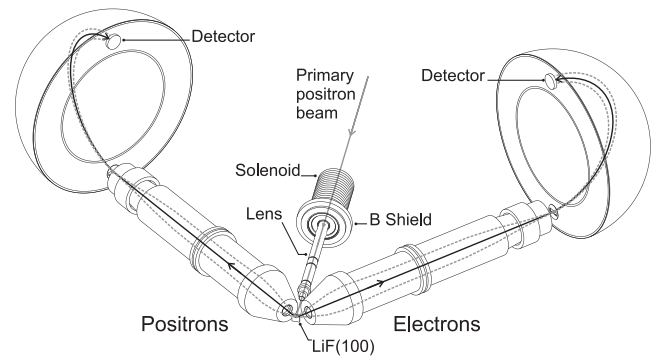


Figure 1. Simplified diagram of the experiment employing two hemispherical analyzers. A primary positron beam is focused onto a LiF(100) surface at normal incidence. The optical axis of each of the transfer lenses are symmetrically positioned in the same plane as the positron beam such that positrons or electrons were detected with a mean angle of 45° with respect to the surface normal.

those that were emitted during a single process on the basis of the time interval between detection of a particle at each of the two detectors. The time interval between the detection of a particle on one detector and the arrival of a second particle on the other detector is measured from signals originating from the multichannel plates that are digitized after amplification and constant fraction discrimination.

Correlated pairs, or *true coincidences*, are emitted during a single process that occurs on a timescale much shorter than the experimental time resolution. The process of most interest that produces correlated pairs is a single scattering event. Multiple scattering events may also occur on a timescale much smaller than the instrumental time resolution. These can generally be distinguished on the basis of the energy of the pair. The measured time interval between the detection of particles comprising a correlated pair shows a finite distribution over a time range that is characteristic of the instrument time resolution. Uncorrelated pairs, or *accidental coincidences* are also detected. These involve two particles which originate from different ionization events, predominantly from electrons emitted following interaction with two different primary positrons. The significance of such events is minimized by using a low primary positron intensity because their rate shows a quadratic dependence on the primary flux, whereas the rate of true coincidences shows a linear dependence. However, the rate of accidental coincidences can also be simply distinguished without varying the primary flux as they are detected with a randomly distributed time interval. Therefore we recorded events for which a pair was detected within a time interval of 150 ns to allow the accidental rate to be estimated and the true coincident rate to be clearly distinguished. We have verified this approach and the correct performance of the instrument by studying the electron pair emission via electron impact both in the laboratory and after installation of the spectrometer at the NEPOMUC beamline. A more detailed account of the instrument will be given elsewhere [19]. The total data acquisition time for the positron experiment was 62 h.

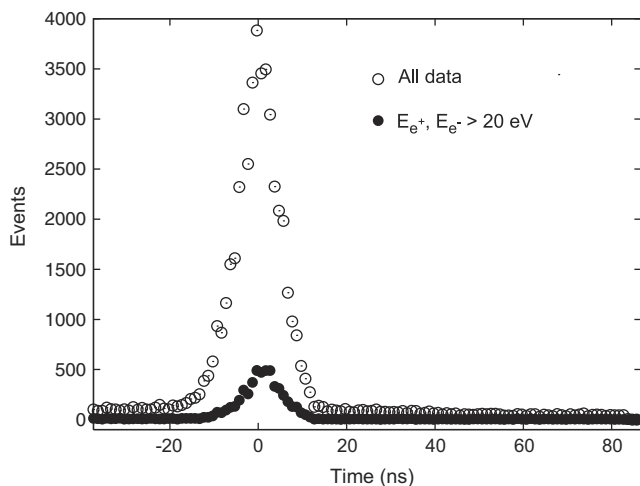


Figure 2. Intensity versus arrival time differences for all detected electron–positron pairs (open circles) and for a subset of the same data that includes only pairs for which the positron and electron were detected with kinetic energy greater than 20 eV (solid circles). The peak in the data is indicative of time-correlated pair emission of positron–electron pairs upon impact with 85 eV positrons.

3. Results

In figure 2 we show the time interval distribution for all detected positron–electron pairs (open circles). A clear peak is present on an essentially constant background. We emphasize that the presence of this peak is evidence of correlated emission of positron–electron pairs from the LiF(100) surface. The area of the peak is a factor of about 20 larger than the area of the background upon which it is superimposed. This very high ratio clearly suggests that an acceptable ratio of true to random coincidences would be maintained with much higher primary positron intensity. The FWHM of the peak, approximately 10 ns, is determined by the time resolution of the instrument, which includes a kinetic energy dependence due to variations in the flight time from the sample to the detector. No attempt has been made to correct the data for this effect as it is accompanied by a flight-time dependency on the angle at which a particle is emitted, and more significantly, on the angle at which the particle enters the hemispherical analyzer. The width is in good agreement with that observed for electron pair emission upon electron impact from the same surface under similar conditions. Our electron–optical simulations also confirm this interpretation qualitatively and quantitatively. To facilitate the discussion that follows we have also shown in figure 2 the time interval distribution for a subset of data that includes only data for which both the electron and positron were detected with a kinetic energy greater than 20 eV. The peak in this data is slightly narrowed and shifted with respect to the peak for the complete data in accordance with energy dependence of the coincidence timing.

We now turn our attention to the energy distribution of the time-correlated electron–positron pairs. The detected intensity of positron–electron pairs increases rapidly from sum energy $E_{\text{sum}} = E_{e^+} + E_{e^-}$ of approximately 60 eV toward lower sum energy. However, our interest lies in the positron–electron

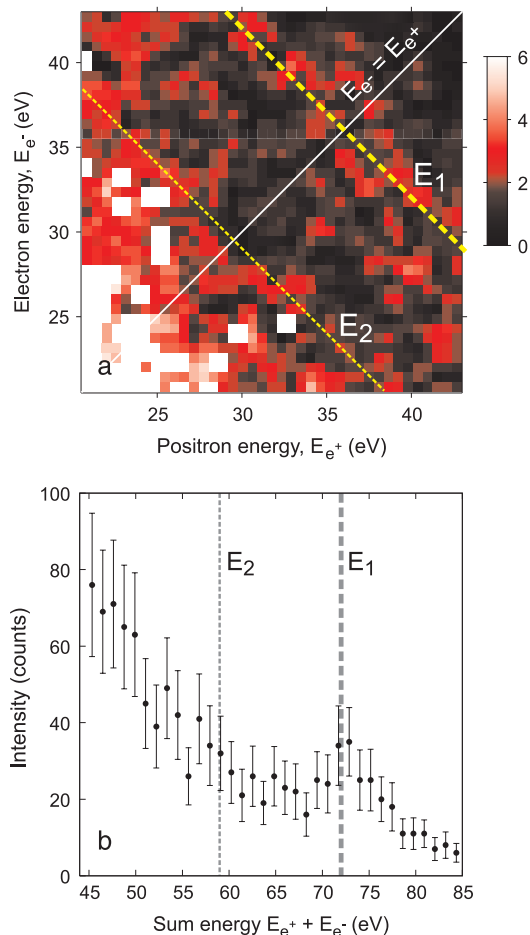


Figure 3. (a) Energy distribution of positron–electron pairs emitted from LiF(100) upon 85 eV positron impact. The intensity indicates the number of correlated pairs detected for each electron and positron energy combination. Only part of the total energy range measured is shown. (b) The positron–electron pair sum energy (E_{sum}) distribution which is the integrated intensity along a 10.3 eV wide strip centred along the line $E_{e^+} = E_{e^-}$ shown in (a). E_1 and E_2 label respectively the maximum sum energy for correlated pair emission and the maximum sum energy available to pair if a participating particle loses energy by an electronic excitation that transfers a valence electron into the conduction band.

energy distribution at higher sum values that are associated with elastic processes involving electrons in the LiF valence band. For analysis of the energy distribution in this region we consider only events for which the time difference is within ± 10 ns of the peak centroid in the subset of the data for which E_{e^+} and E_{e^-} are both greater than 20 eV, i.e. the data within the peak shown with solid circles in figure 2. This selection contains very few accidental coincidences. A two-dimensional energy spectrum, E_{e^+} versus E_{e^-} , constructed from the selected events is shown in figure 3(a). A weak ridge can be seen that along $E_{\text{sum}} \approx 72$ eV. This feature, labelled E_1 in figure 3(a), is the central result of this work. It is revealed more clearly in figure 3(b) which shows the integrated intensity along a 10.3 eV wide strip centred along the line $E_{e^+} = E_{e^-}$, indicated by the solid white line in figure 3(a), against the sum energy $E_{\text{sum}} = E_{e^+} + E_{e^-}$.

The significance of the feature at 72 eV in the sum energy distribution can be understood from a simple consideration of energy conservation that requires that the maximum sum energy for correlated positron–electron pairs to be given by the primary positron energy minus the energy required to emit an electron from the top of the valence band. Because the conduction band is close to the vacuum level in LiF, the latter quantity is essentially the band gap, which is 13.0 ± 0.4 eV [7]. Therefore the upper limit for E_{sum} in the present experiment is 72 eV, which is in close agreement with the position of the peak in the sum energy distribution. The peak can therefore be attributed to scattering events that involve an 85 eV primary positron with an electron from the top of the valence band. A corresponding feature is observed in the sum energy distribution of electron pairs under electron impact with the same apparatus and with previous experiments [15]. We emphasize that this feature is not observed in single particle spectroscopy because the energy of the single electrons detected is not constrained by the energy conservation condition described above. The feature at 72 eV sum energy in the present experiment is therefore the definitive evidence that correlated positron–electron pairs are emitted from a surface under positron impact.

The continuously increasing intensity below about 60 eV, excluded from figure 3, can be attributed to inelastic processes. If an electronic excitation transfers a valence electron into the conduction band, the maximum sum energy available will be reduced by the band gap energy of 13–59 eV. This position is labelled E_2 in figure 3. The inelastic processes that slow a positron implanted in wide band gap materials like LiF have been broadly discussed in the context of positron remission and positronium emission [17, 21, 22]. It is generally accepted that positron energy loss is dominated by production of collective electronic excitations and by electron–hole pair and exciton formation until the positron energy falls below the band gap and these processes are no longer energetically possible [17]. As with electrons, a low kinetic energy positron beam also undergoes diffraction at a crystal surface [16, 21, 23, 24]. The intensity of a Bragg peak observed for a positron energy close to that of our primary beam has been reported to be only about 0.1% of the primary intensity [16]. This is consistent with our own observations and partly explains the relatively low intensity of the peak at $E_{\text{sum}} = 72$ eV in the energy spectrum shown in figure 3.

The charged particle optics and detection scheme employed in the experiment allow the emission angle of the detected particles to be measured simultaneously with the kinetic energy, albeit with significant reduction in detection efficiency. Such a mode of operation, which is of course necessary for a momentum resolved pair emission experiment, was not used because beamtime was limited and countrates were low. Our experience with electron–electron pair emission shows that counting statistics will generally impose a practical limit on the effective energy and angular resolution. This is because the energy and angular distribution recorded by one detector must be partitioned in such a way that each partition includes sufficient data to allow statistically meaningful analysis of the corresponding (coincident) distribution seen

by the second detector. To achieve an acceptable effective energy and angular resolution we require an increase in count-rate and acquisition time. The data indicate that we would have measured an acceptable ratio of true coincidences to accidental coincidences with a primary positron intensity a factor of twenty greater. We are currently in the process of improving our experimental apparatus to make this possible while minimizing the positron beam area (which affects energy and angular resolution). It has been demonstrated that NEPOMUC beamline can deliver substantially more intensity than we require [25]. We conclude that a momentum resolved experiment is therefore viable.

4. Summary

We have shown that the correlated emission of positron–electron pairs from solid surfaces occurs. Upon impact with 85 eV positrons, positron–electron pairs were detected from a LiF(100) surface with a weak peak in the pair energy distribution at approximately 72 eV that is attributed to the primary positron scattering with an electron from the top of the valence band. These observations demonstrate the viability of performing momentum resolved measurements of the positron–electron pair distribution upon positron impact.

Acknowledgments

We acknowledge the dedicated effort by the NEPOMUC team, lead by Dr C Hugenschmidt, to make the beamline available.

References

- [1] Berakdar J 1998 *Phys. Rev. B* **58** 9808
- [2] Berakdar J, Gollisch H and Feder R 1999 *Solid State Commun.* **112** 587
- [3] Feder R, Gollisch H, Meinert D, Scheunemann T, Artamonov O M, Samarin S N and Kirschner J 1998 *Phys. Rev. B* **58** 16418
- [4] Fominykh N, Henk J, Berakdar J, Bruno J, Gollisch J and Feder R 2000 *Solid State Commun.* **113** 665
- [5] Gollisch H, Schwartzberg N v and Feder R 2006 *Phys. Rev. B* **74** 075407
- [6] Kirschner J, Artamonov O M and Samarin S N 1995 *Phys. Rev. Lett.* **75** 2424
- [7] Samarin S, Artamonov O M, Suvorova A A, Sergeant A D and Williams J F 2004 *Solid State Commun.* **129** 389
- [8] Schumann F O, Kirschner J and Berakdar J 2005 *Phys. Rev. Lett.* **95** 117601
- [9] Schumann F O, Winkler C and Kirschner J 2007 *New J. Phys.* **9** 372
- [10] Schumann F O, Winkler C and Kirschner J 2007 *Phys. Rev. Lett.* **98** 257604
- [11] Wigner E and Seitz F 1933 *Phys. Rev.* **43** 804
- [12] Slater J C 1951 *Phys. Rev.* **81** 385
- [13] Berakdar J 2000 *Nucl. Instrum. Methods Phys. Res. B* **171** 204
- [14] Hugenschmidt C, Schreckenbach K, Stadlbauer M and Straßer B 2005 *Nucl. Instrum. Methods Phys. Res. A* **554** 384
- [15] Samarin S, Berakdar J, Suvorova A, Artamonov O M, Waterhouse D K, Kirschner J and Williams J F 2004 *Surf. Sci.* **548** 187
- [16] Mills A P and Crane W S 1985 *Phys. Rev. B* **31** 3988
- [17] Tuomisaari M, Howell R H and McMullen T 1989 *Phys. Rev. B* **40** 2060

- [18] Goodyear A and Coleman P G 1995 *Meas. Sci. Technol.* **6** 415
- [19] van Riessen G, Birke M, Winkler C, Schumann F O and Kirschner J 2008 in preparation
- [20] Hugenschmidt C, Brunner T, Legl S, Mayer J, Piochacz C, Stadlbauer M and Schreckenbach K 2007 *Phys. Status Solidi c* **4** 3947
- [21] Schultz P J and Lynn K G 1988 *Rev. Mod. Phys.* **60** 701
- [22] Mills A P and Crane W S 1984 *Phys. Rev. Lett.* **53** 2165
- [23] Rosenberg I J, Weiss A H and Canter K F 1980 *Phys. Rev. Lett.* **44** 1139
- [24] Weiss A H, Rosenberg I J, Canter K F, Duke C B and Paton A 1983 *Phys. Rev. B* **27** 867
- [25] Hugenschmidt C, Löwe B, Mayer J and Piochacz C 2008 *Nucl. Instrum. Methods Phys. Res. A* **593** 616–8